

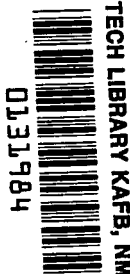
NASA TECHNICAL NOTE



NASA TN D-5216

c.1

LOAN COPY: RETURN
AFWL (WLIL-2)
KIRTLAND AFB, N ME



NASA TN D-5216

STUDY OF THE (α , t) REACTION ON SCANDIUM-45 AT 41 MeV

by

Joseph R. Priest
Miami University

and

John S. Vincent
Lewis Research Center



STUDY OF THE (α ,t) REACTION ON SCANDIUM-45 AT 41 MeV

By Joseph R. Priest

Physics Department
Miami University
Oxford, Ohio

and John S. Vincent

Lewis Research Center
Cleveland, Ohio

NATIONAL AERONAUTICS AND SPACE ADMINISTRATION

For sale by the Clearinghouse for Federal Scientific and Technical Information
Springfield, Virginia 22151 - CFSTI price \$3.00

ABSTRACT

Thirteen angular distributions have been measured from 8° to 70° for the $\text{Sc}^{45}(\alpha, t)\text{Ti}^{46}$ reaction at 41 MeV. All exhibit the same basic shape, which is consistent with a distorted wave calculation where three units of angular momentum are transferred. Relative spectroscopic strengths for these transitions agree well with experimental values obtained by others for the (He^3, d) reaction. Good overall agreement is obtained in a comparison with spectroscopic factors calculated from the McMullen, Bayman, and Zamick model for Sc^{45} and Ti^{46} .

STUDY OF THE (α , t) REACTION ON SCANDIUM-45 at 41 MeV

by Joseph R. Priest* and John S. Vincent

Lewis Research Center

SUMMARY

Thirteen angular distributions have been measured from 8° to 70° for the (α , t) reaction on scandium-45 at 41 MeV. Very selective population of the states of Ti^{46} was observed, and these correlate well with those of the $\text{Sc}^{45}(\text{He}^3, \text{d})\text{Ti}^{46}$ reaction which have large spectroscopic strengths for an orbital angular momentum transfer of three units ($l_p = 3$). The angular distributions have little structure and exhibit the same basic shape. The distorted wave Born approximation noncutoff calculations for the stripping of an $l_p = 3$ proton provides an adequate description of the angular distributions. The relative spectroscopic strengths extracted from the distorted wave Born approximation analysis agree favorably with those deduced from a similar study of the $\text{Sc}^{45}(\text{He}^3, \text{d})\text{Ti}^{46}$ reaction. Theoretical spectroscopic strengths calculated from the McCullen, Bayman, and Zamick single-particle wave functions for the ground state of Sc^{45} and five low-lying states of Ti^{46} are in reasonable agreement with experiment.

INTRODUCTION

The study of reactions where a single nucleon is transferred from a projectile to a target can yield information which is rich in details of the nuclear structure. The success in extracting this information depends, however, on the extent to which the mechanism of the reaction is understood. Of the proton transfer reactions (d, n) and (He^3, d) have generally been characterized as stripping processes and have been compared with direct-reaction theories such as the distorted wave Born approximation (DWBA). Analysis of a few (α , t) reactions using current DWBA stripping theories have been less successful (refs. 1 to 4); even though at sufficiently high incident energy, the angular distributions have many of the attributes of the other reactions. The interpretation has been

*Physics Department, Miami University, Oxford, Ohio 45056.

that the (α, t) process is direct but not entirely of the stripping type. The principal difference between the (α, t) reaction and the (d, n) and (He^3, d) proton-transfer reactions is that high angular momentum transfers are favored in the (α, t) process. This condition is attributed to the momentum mismatch and, at medium incident energies, results in the preferential population of residual states requiring three to five units of transferred angular momentum (refs. 5 and 6). The choice of a suitable target to study the (α, t) reaction as a spectroscopic tool should be governed by the following considerations: (1) the nucleus should have structure which is well understood from independent model calculations and (2) there should be an abundance of states for which the orbital angular momentum of the captured proton is three or four. Nuclei with protons in the $1f_{7/2}$ shell satisfy this requirement. The $\text{Sc}^{45}(\alpha, t)\text{Ti}^{46}$ reaction is particularly suited because reasonable model wave functions are available (ref. 7), and two studies of the $\text{Sc}^{45}(\text{He}^3, d)\text{Ti}^{46}$ reaction are available for comparison (refs. 8 and 9). The results of an investigation of the (α, t) reaction on Sc^{45} using 41 MeV alpha particles are reported in this paper.

SYMBOLS

A	atomic number
a	nuclear diffuseness
C	Clebsch-Gordon coefficient
$D^{\alpha J_f}, C^{\beta J_L}$	components of normalized eigenvectors for the α^{th} state in target and β^{th} state in residual
$d\sigma/d\Omega$	differential cross section
J_f	spin of final state
J_i	spin of initial state
k_i, k_α	incident wave vector
k_f, k_t	exit wave vector
L_n, L_p	angular momentum quantum number of coupled Z-20 neutrons and N-20 protons
l_p	orbital angular momentum quantum number of transferred proton
M_R	mass of the residual nucleus
M_T	mass of target
N	number of data points

n	number of equivalent nucleons of type transferred in residual nucleus
\vec{q}	momentum transfer vector
R	nuclear radius
r_0	reduced nuclear radius
S_l	spectroscopic factor
t_n	n^{th} state excited in this study
U	normalized Racah coefficient in Jahn's (ref. 24) notation
V	real nuclear potential
V_C	Coulomb potential for uniformly charged sphere of radius $r_0 A^{1/3}$
W	imaginary nuclear potential
γ	normalization parameter for comparing experimental and theoretical reaction cross sections
ν	seniority quantum number
σ_{DWBA}	differential cross section calculated from distorted wave Born approximation
σ^{exp}	experimental differential cross section
σ^{theo}	theoretical differential cross section
$\Delta\sigma^{\text{exp}}$	experimental error
φ_m^j	single particle wave function of captured nucleon
χ_n^2	usual measure of goodness of fit between experimental and theoretical data
ψ_M^J	nuclear wave functions having total angular momentum J and Z component M

EXPERIMENTAL PROCEDURES AND RESULTS

The Lewis Research Center fixed-energy cyclotron provided the source of 41.0 ± 0.2 MeV alpha particles. The Sc^{45} target was a self-supporting, evaporated film having an areal density of 0.926 ± 0.050 milligram per square centimeter. The tritons were detected in a 4.5-millimeter-thick lithium drifted silicon detector. The defining aperture of this counter was rectangular and subtended a solid angle of 1.24×10^{-4} steradian. Tritons were discriminated from other $Z = 1$ reaction products by a ΔE - E counter telescope and a particle identifier similar to the design of Goulding et al. (ref. 10). The effectiveness of this system can be assessed from the mass spectrum shown in figure 1. A triton spectrum for a laboratory angle of 20° is shown by the open

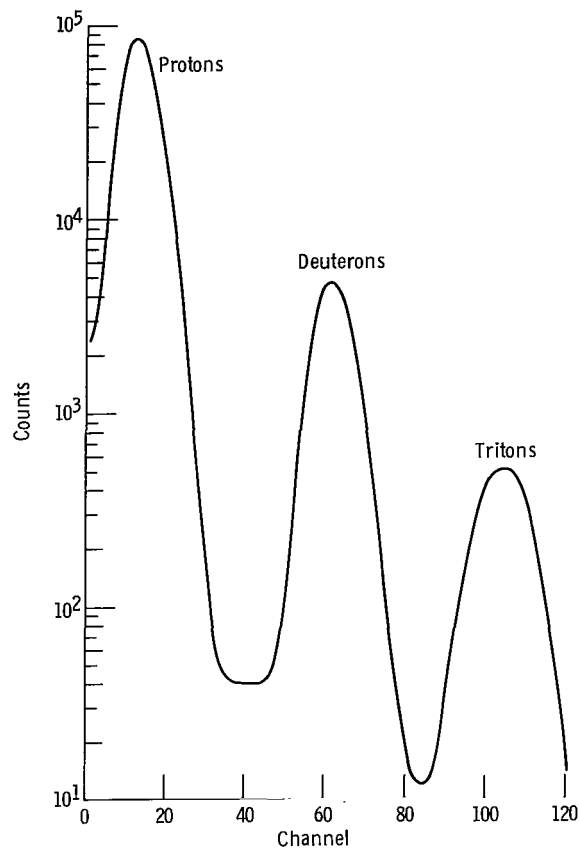


Figure 1. - Mass identifier output spectrum for $Z = 1$ reaction products.

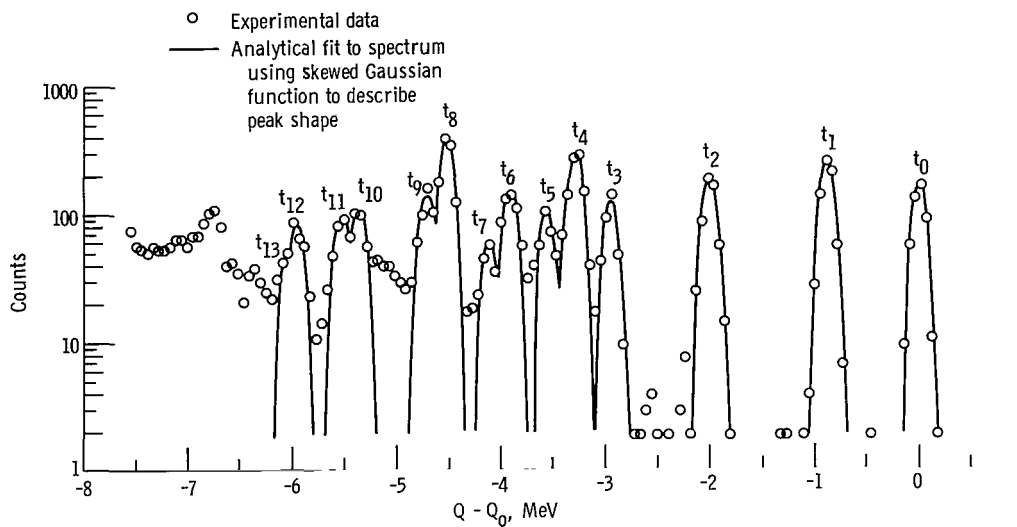


Figure 2. - Triton spectrum obtained at 20° for $\text{Sc}^{45}(\alpha, t)\text{Ti}^{46}$ reaction at 41 MeV. Calibration curve used to calculate excitation energies shown is based on linear least squares fit between Q -values and peak positions obtained from computer fits to spectra for t_0 , t_1 , t_2 , and t_8 groups. (The Q -values for these four excitations were taken from ref. 8).

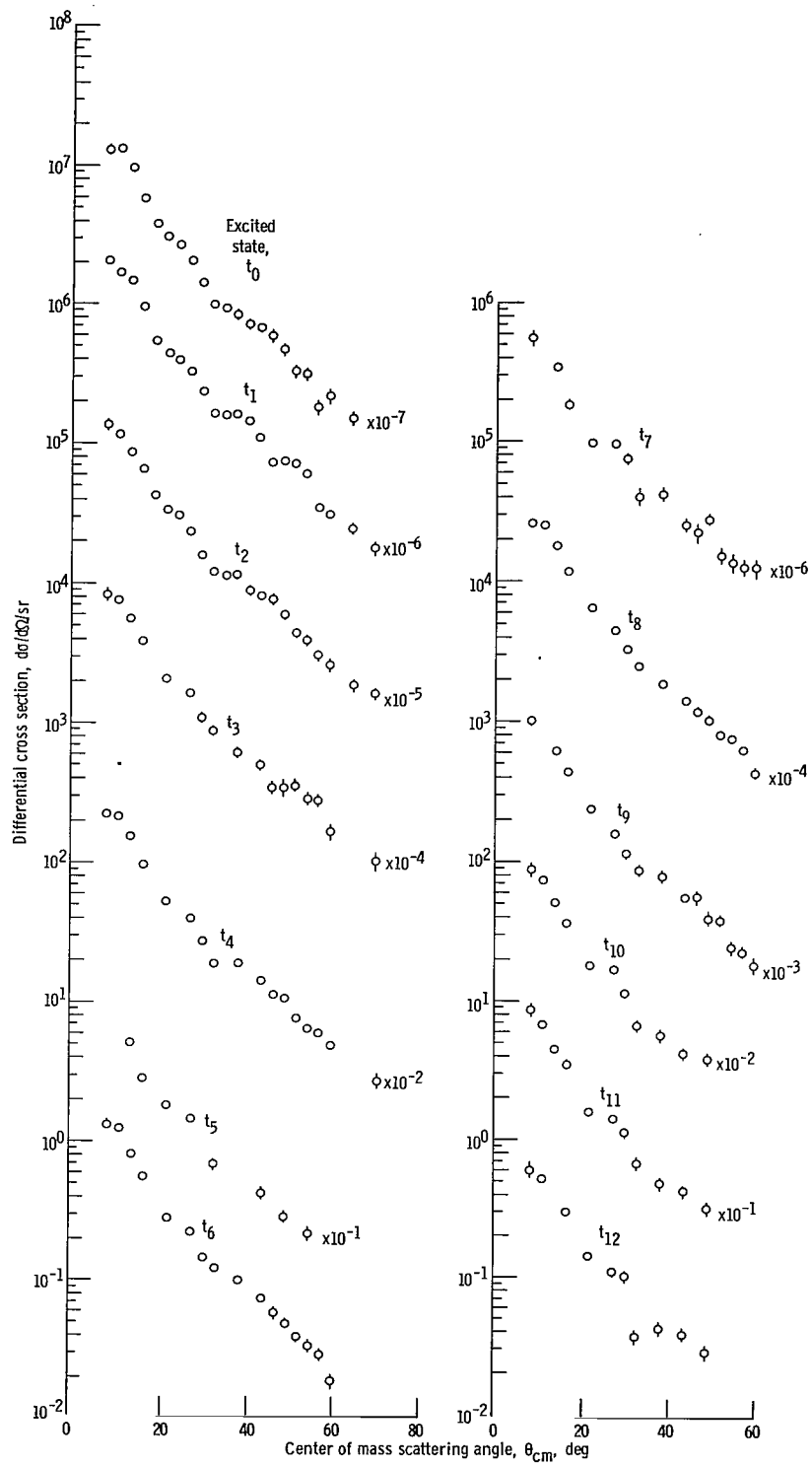


Figure 3. - Summary of measured triton angular distributions for $\text{Sc}^{45}(\alpha, t)\text{Ti}^{46}$ reaction at 41 MeV. Errors shown are due only to statistical uncertainties. The t_1 notation refers to the triton group designated in figure 2. The mean excitation energies in titanium-46 corresponding to these groups can be inferred from table III.

TABLE I. - NUMERICAL DATA

Scattering angle, θ , deg	Differential cross section, $d\sigma/d\Omega$, $\mu\text{b/sr}$	Experimental error, $\Delta\sigma$, $\mu\text{b/sr}$	Scattering angle, θ , deg	Differential cross section, $d\sigma/d\Omega$, $\mu\text{b/sr}$	Experimental error, $\Delta\sigma$, $\mu\text{b/sr}$	Scattering angle, θ , deg	Differential cross section, $d\sigma/d\Omega$, $\mu\text{b/sr}$	Experimental error, $\Delta\sigma$, $\mu\text{b/sr}$
Excited state, t_0			Excited state, t_2			Excited state, t_4		
8.2	1283.8	118.7	8.2	1363.6	122.0	8.2	2194.7	154.5
10.9	1327.2	48.3	10.9	1162.9	45.0	11.0	2110.1	60.5
13.6	969.9	41.5	13.7	862.1	39.0	13.7	1539.9	52.0
16.3	573.4	32.1	16.4	655.4	34.2	16.4	964.2	40.3
19.1	378.6	18.4	19.1	419.8	19.3	21.9	518.7	17.2
21.8	305.5	13.3	21.8	332.8	13.8	27.3	395.2	15.3
24.5	266.3	14.1	24.5	303.5	15.1	30.0	268.6	13.9
27.2	204.4	11.0	27.2	233.9	11.8	32.7	185.9	11.0
29.9	140.9	10.1	30.0	155.9	10.6	38.1	185.4	10.8
32.6	99.0	8.1	32.7	119.4	8.9	43.5	137.7	7.4
35.2	92.5	7.2	35.3	111.4	7.9	46.2	110.2	8.8
37.9	83.5	7.3	38.0	114.3	8.5	48.8	104.2	6.6
40.6	70.2	6.5	40.7	86.9	7.2	51.5	74.7	5.3
43.3	66.4	5.2	43.4	79.5	5.6	54.1	63.1	4.6
45.9	58.0	6.4	46.1	75.4	7.3	56.8	58.2	3.7
48.6	46.5	4.4	48.7	58.2	4.9	59.4	47.8	3.9
51.3	32.3	3.5	51.4	42.4	4.0	69.9	25.8	2.6
53.9	30.7	3.2	54.0	38.3	3.6	Excited state, t_5		
56.5	18.0	2.1	56.7	30.0	2.7	13.7	508.8	29.9
59.2	21.5	2.7	59.3	25.8	2.9	16.4	282.8	22.4
64.4	14.8	1.8	64.6	18.3	2.0	21.9	179.8	10.1
69.6	5.9	1.3	69.8	15.6	2.0	27.3	144.5	9.2
Excited state, t_1			Excited state, t_3			32.7	67.6	6.7
8.2	2046.8	149.7	8.2	826.6	94.9	43.5	42.4	4.1
10.9	1675.0	54.1	11.0	760.3	36.4	48.8	27.8	3.4
13.6	1460.9	50.9	13.7	555.5	31.3	54.2	21.1	2.7
16.4	946.2	41.1	16.4	387.9	26.3			
19.1	536.4	21.9	21.9	206.7	10.9			
21.8	437.5	15.8	27.3	159.4	9.7			
24.5	393.7	17.2	30.0	107.7	8.8			
27.2	320.7	13.8	32.7	86.6	7.6			
29.9	230.2	12.9	38.1	60.4	6.2			
32.6	160.3	10.3	43.5	49.5	4.5			
35.3	157.3	9.4	46.1	33.8	4.9			
38.0	159.0	10.0	48.8	34.0	3.8			
40.7	143.7	9.2	51.5	35.4	3.6			
43.3	107.3	6.6	54.1	28.5	3.3			
46.0	72.0	7.2	56.8	27.4	2.6			
48.7	72.7	5.5	59.4	16.4	2.3			
51.3	69.6	5.1	69.9	10.2	1.7			
54.0	59.9	4.5						
56.6	33.8	2.9						
59.2	30.3	3.1						
64.5	24.1	2.3						
69.7	17.4	2.2						

TABLE I. - Concluded. NUMERICAL DATA

Scattering angle, θ , deg	Differential cross section, $d\sigma/d\Omega$, $\mu\text{b/sr}$	Experimental error, $\Delta\sigma$, $\mu\text{b/sr}$	Scattering angle, θ , deg	Differential cross section, $d\sigma/d\Omega$, $\mu\text{b/sr}$	Experimental error, $\Delta\sigma$, $\mu\text{b/sr}$	Scattering angle, θ , deg	Differential cross section, $d\sigma/d\Omega$, $\mu\text{b/sr}$	Experimental error, $\Delta\sigma$, $\mu\text{b/sr}$
Excited state, t_6			Excited state, t_8			Excited state, t_{10}		
8.2	1333.6	120.3	8.3	2574.9	167.0	8.3	862.9	96.5
11.0	1240.6	46.4	11.0	2520.8	66.0	11.0	723.0	35.3
13.7	804.3	37.6	13.7	1767.8	55.6	13.7	496.9	29.5
16.4	554.4	31.3	16.5	1180.4	45.7	16.5	353.1	25.0
21.9	273.8	12.5	21.9	633.9	18.9	21.9	175.3	10.0
27.3	219.1	11.4	27.4	438.9	16.0	27.4	164.0	9.8
30.0	142.9	10.1	30.1	321.5	15.2	30.1	110.4	8.9
32.8	118.8	8.8	32.8	243.5	12.6	32.8	64.6	6.5
38.2	95.7	7.8	38.2	182.9	10.7	38.2	55.1	5.9
43.5	70.9	5.3	43.6	139.2	7.4	43.6	41.0	4.0
46.2	55.4	6.3	46.2	117.6	9.1	49.0	37.4	3.9
48.9	47.0	4.4	48.9	103.5	6.5	Excited state, t_{11}		
51.5	37.5	3.7	51.6	79.6	5.4	8.3	862.4	96.5
54.2	32.0	3.3	54.2	74.6	5.0	11.0	672.6	34.1
56.8	27.6	2.6	56.9	62.0	3.8	13.8	446.0	27.9
59.5	17.9	2.4	59.5	42.6	3.7	16.5	347.6	24.8
Excited state, t_7			Excited state, t_9			22.0	157.2	9.4
8.3	563.4	78.2	8.3	1016.3	104.9	27.4	140.1	9.1
11.0	534.3	30.4	11.0	814.4	37.5	30.1	111.1	8.9
13.7	352.0	24.9	13.7	606.4	32.6	32.8	67.2	6.6
16.4	188.8	18.3	16.5	431.4	27.6	38.3	47.6	5.5
21.9	98.8	7.5	21.9	234.8	11.5	43.6	42.1	4.1
27.3	98.7	7.6	27.4	157.4	9.6	49.0	31.7	3.6
30.1	75.4	7.4	30.1	112.1	9.0	Excited state, t_{12}		
32.8	40.9	5.2	32.8	85.5	7.5	8.3	602.7	80.6
38.2	42.2	5.2	38.2	76.2	6.9	11.0	518.7	29.9
43.5	25.1	3.2	43.6	53.6	4.6	16.5	299.8	23.0
46.2	22.5	4.0	46.3	54.6	6.2	22.0	144.7	9.1
48.9	28.2	3.4	48.9	38.3	4.0	27.4	109.7	8.0
51.6	15.3	2.4	51.6	37.8	3.8	30.2	101.0	8.5
54.2	13.6	2.1	54.3	23.9	2.8	32.9	37.4	5.0
56.9	12.8	1.8	56.9	22.5	2.3	38.3	43.2	5.2
59.5	12.6	2.0	59.6	17.9	2.4	43.7	39.0	3.9
						49.0	28.9	3.5

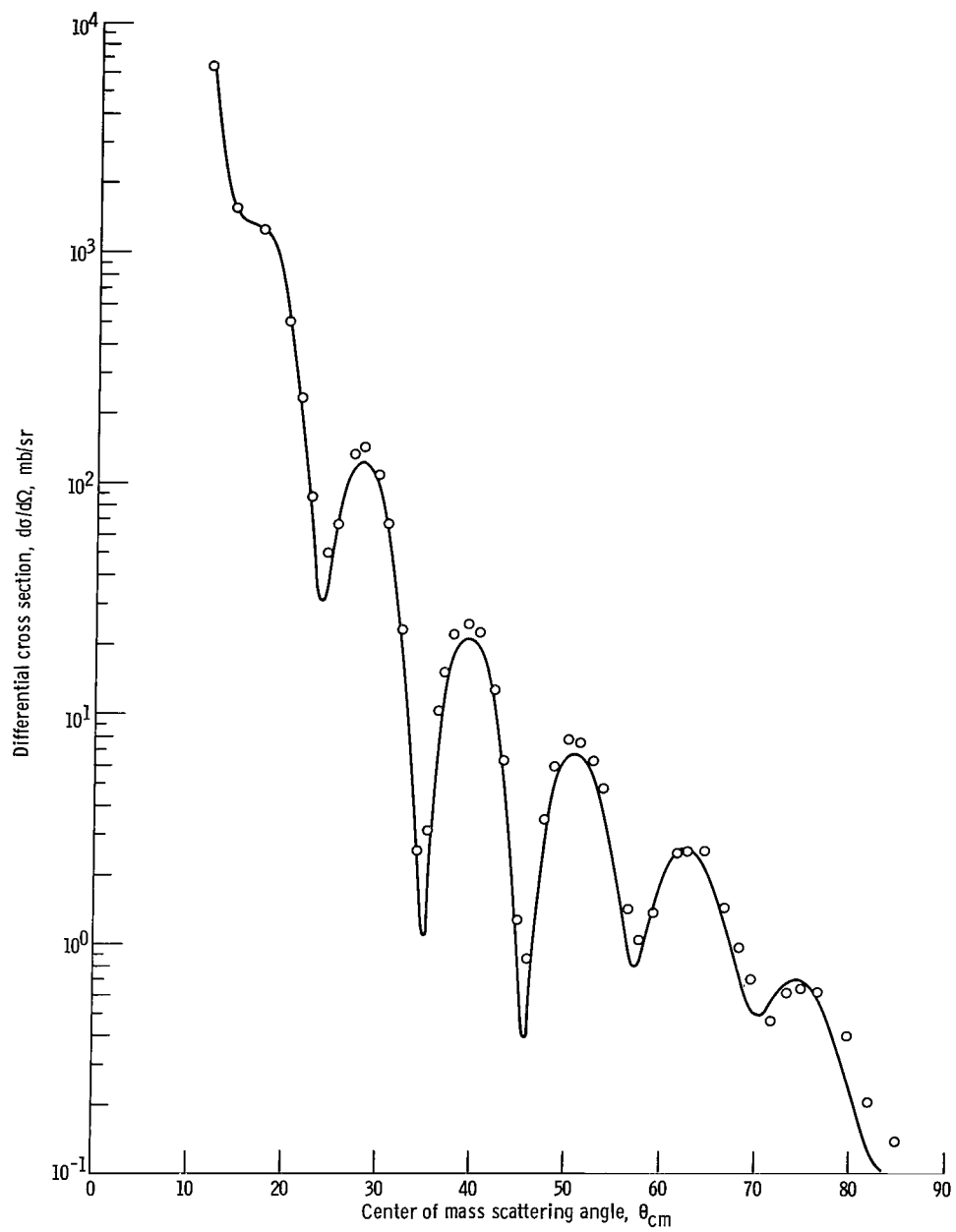


Figure 4. - Optical model fit to $Sc^{45}(\alpha, \alpha)Sc^{45}$ angular distribution for alpha-particle energy of 41 MeV. Parameters used were set 4 (table IV). Fits obtained with the sets of parameters shown in table IV were practically indistinguishable.

circles in figure 2. An evaluation of this spectrum yields an overall energy resolution of 150 keV full width at half maximum.

The first three triton groups in figure 2 are completely resolved and correspond to production of the ground and first two excited states of Ti^{46} (ref. 11). There are also a number of prominent, but only partially resolved groups in the spectrum. These groups more than likely do not correspond to excitation of a discrete state but do represent preferential production of a state. They were analyzed by the following procedure: For each angle the three resolved groups were fitted with a skewed Gaussian function using a least-squares computer program. This procedure yielded the width parameter, peak position, and areas under the curve of the Gaussian function. An average value of the width

TABLE II. - DIFFERENTIAL CROSS SECTIONS FOR
ELASTIC SCATTERING OF 41-MeV ALPHA
PARTICLES FROM SCANDIUM-45

Scattering angle, θ , deg	Differential cross section, $d\sigma/d\Omega$, mb/sr	Scattering angle, θ , deg	Differential cross section, $d\sigma/d\Omega$, mb/sr
11.97	6494	45.94	0.846
14.69	1565	47.54	3.45
17.40	1256	48.60	5.83
20.12	505.7	50.20	7.63
21.74	234.2	51.26	7.26
22.83	86.56	52.85	6.16
24.45	49.88	53.90	4.62
25.53	67.76	56.54	1.30
27.15	130.4	57.60	1.02
28.23	132.6	59.18	1.35
29.85	107.5	61.80	2.44
30.93	65.84	62.85	2.43
32.55	22.92	64.42	2.51
34.16	2.55	66.50	1.43
35.24	3.07	68.06	.953
36.31	10.17	69.62	.586
36.85	14.93	71.69	.452
37.92	21.80	73.24	.588
39.53	24.08	74.79	.617
40.60	22.10	76.85	.611
42.21	12.51	79.93	.387
43.28	6.21	81.97	.203
44.88	1.26	85.02	.133

parameter for the three fits was extracted, and this value was held fixed for the fitting of the remaining prominent triton groups. Typical results using this method are illustrated by the solid line in figure 2. The standard deviation between computer calculation and the total number of counts obtained by summing 66 resolved spectral peaks was calculated to be 5.5 percent. Differential cross sections for production of the states labeled t_0 to t_2 were calculated using triton yields obtained by summing the counts in the groups. Those for the states labeled t_3 to t_{12} were calculated using the yields obtained from the computer fits. The overall uncertainty in the cross sections for these two sets is assessed at 15 and 25 percent, respectively. The uncertainty in the relative cross sections is estimated as 10 and 20 percent since a fixed monitor counter was used to normalize the data. The center-of-mass differential cross sections plotted against the center-of-mass reaction angle are presented in figure 3. The errors shown reflect only the statistical uncertainty in the cross sections. The numerical data are presented in table I.

In addition to the reaction cross sections, the elastic scattering of alpha particles by Sc^{45} was measured using the same target. This was necessary to obtain a description of the incident channel. The data are shown in figure 4 and in table II.

DISCUSSION

Several studies of the states of Ti^{46} have been reported (refs. 8, 9, and 12 to 17). The most useful of these for the present study are those of Mo et al. (ref. 17) who studied the $\text{Ti}^{46}(\text{p}, \text{p}'\gamma)\text{Ti}^{46}$ reaction, and Broman and Pullen (ref. 8) and Barnard and Jones (ref. 9), who studied the $\text{Sc}^{45}(\text{He}^3, \text{d})\text{Ti}^{46}$ reaction. Their results are summarized in the first seven columns of table III. The mean Ti^{46} excitation energies for our study are listed in the eighth column. These were obtained from the analytic form of an energy calibration curve based on a linear least squares fit between the Q-values and peak positions obtained from the computer fits to the spectra for the t_0 , t_1 , t_2 , and t_8 groups. Those states designated in the eighth column of table III correlate well with those states in the $\text{Sc}^{45}(\text{He}^3, \text{d})\text{Ti}^{46}$ reaction having large $l_p = 3$ spectroscopic strengths. This is expected from the momentum-mismatch argument which can be formulated as follows. The momentum-transfer vector for a stripping reaction is defined as

$$\mathbf{q} \equiv \mathbf{k}_i - \frac{M_T}{M_R} \mathbf{k}_f \quad (1)$$

where \mathbf{k}_i and \mathbf{k}_f are the center-of-mass wave vectors of the incident and exit particles and M_T and M_R are the masses of the target and residual nuclei. The momentum

TABLE III. - SUMMARY OF PERTINENT SPECTROSCOPIC INFORMATION FOR TITANIUM-46

Source									
Ref. 17	Ref. 9			Ref. 8			Present investigation		
Excitation, ^a MeV	Excitation, MeV	L-transfer	Spectroscopic strength	Excitation, ^b MeV	L-transfer	Spectroscopic strength	Excitation, ^c MeV	Triton group ^d	Spectroscopic strength
0	0	3	0.27	0	3	0.53	0	t-0	0.27
.89	.887	1,3	0.06+0.28	.891	1,3	0.25+0.96	.890	t-1	.40
2.01	2.006	1,3	.04+0.22	2.014	1,3	.20+0.72	2.012	t-2	.30
2.61	---	---	---	---	---	---	---	---	---
2.96	2.96	3	.22	2.974	3	.50	2.963	t-3	.20
3.06	---	---	---	3.074	2	.09	---	---	---
3.17	3.17	3	.58	---	---	---	---	---	---
3.23	---	---	---	3.247	1,3	.01+0.24	---	---	---
3.29	---	---	---	3.310	3	.90	3.294	t-4	.55
3.44	3.44	3	.16	3.455	2	.27	---	---	---
3.58	---	---	---	3.598	1,3	.02+0.36	3.575	t-5	.20
3.73	---	---	---	3.737	1	.06	---	---	---
---	---	---	---	3.861	1,3	.06+0.31	---	---	---
3.90	3.90	1,3	.09+0.36	---	---	---	3.920	t-6	.33
---	---	---	---	3.955	1,3	.09+0.57	---	---	---
4.05	---	---	---	4.049	1	.08	---	---	---
---	---	---	---	4.158	1,3	.02+0.14	4.133	t-7	.14
4.21	---	---	---	4.206	3	.23	---	---	---
4.35	---	---	---	4.394	1	.04	---	---	---
4.45	---	---	---	4.533	3	2.11	4.533	t-8	.76
4.64	---	---	---	4.620	1	.06	---	---	---
4.72	---	---	---	4.723	1,3	.03+0.59	4.733	t-9	.27
4.83	---	---	---	4.846	1,3	.03+0.08	---	---	---
---	---	---	---	4.999	1,3	.01+0.05	---	---	---
---	---	---	---	5.045	0	.06	---	---	---
---	---	---	---	5.098	1	.13	---	---	---
---	---	---	---	5.187	1,3	.02+0.17	---	---	---
---	---	---	---	5.326	1	.02	---	---	---
---	---	---	---	5.383	1,3	.07+0.40	5.370	t-10	.26
---	---	---	---	5.557	1,3	.14+0.41	5.549	t-11	.25
---	---	---	---	5.618	1	.06	---	---	---
---	---	---	---	5.816	0	.06	---	---	---
---	---	---	---	5.899	1,3	.02+0.04	---	---	---
---	---	---	---	5.982	1,3	.02+0.31	5.967	t-12	.22
---	---	---	---	6.029	1	.05	---	---	---
---	---	---	---	6.088	0	.03	---	---	---
---	---	---	---	6.141	1,3	.01+0.08	---	---	---
---	---	---	---	6.214	0	.01	---	---	---
---	---	---	---	5.246	0	0	---	---	---
---	---	---	---	5.335	1	.06	---	---	---
---	---	---	---	6.427	1	.16	---	---	---
---	---	---	---	6.556	1,3	.09+0.22	---	---	---
---	---	---	---	6.623	1	.03	---	---	---
---	---	---	---	6.744	1,3	.13+0.51	---	---	---
---	---	---	---	6.856	1,3	.02+0.33	---	---	---
---	---	---	---	6.897	1	.04	---	---	---
---	---	---	---	6.979	1,3	.02+0.14	---	---	---
---	---	---	---	7.049	1,3	.09+0.18	---	---	---
---	---	---	---	7.101	1	.08	---	---	---
---	---	---	---	7.147	1	.06	---	---	---
---	---	---	---	7.204	1,3	.09+0.20	---	---	---
---	---	---	---	7.294	1	.06	---	---	---
---	---	---	---	7.349	1	.16	---	---	---
---	---	---	---	7.433	1	.25	---	---	---
---	---	---	---	7.565	1	.42	---	---	---

^aExcitation energies from $Ti^{46}(p,p'\gamma)Ti^{46}$. Uncertainty quoted is ± 10 keV.^bUncertainties quoted are ± 12 keV for energies less than 3.955 MeV, ± 15 keV for energies between 4.049 and 5.982 MeV, and ± 20 keV for energies between 6.029 and 7.565 MeV.^cEstimated uncertainty is ± 30 keV.^dLevel designation corresponding to triton groups shown in fig. 2.

transfer vector $|\underline{q}|$ depends not only on $|\underline{k}_i|$ and $|\underline{k}_f|$ but also on the reaction angle. And it is a minimum for a reaction angle of 0, is zero if $\underline{k}_i = (M_T/M_R) \times \underline{k}_f$ (i. e., if the momenta are matched), and increases monotonically with angle. If $|\underline{k}_i|$ and $(M_T/M_R) \times |\underline{k}_f|$ are unequal, the minimum $|\underline{q}|$ can be substantially different from zero. In a simple stripping reaction we expect the maximum in the differential cross section to occur at an angle corresponding to $|\underline{q}| R = l$ where R is the radius of the nuclear surface, and $l\hbar$ is the orbital angular momentum of the transferred nucleon (ref. 18). This is indeed the case for the $\text{Sc}^{45}(\text{He}^3, d)\text{Ti}^{46}$ data (ref. 17). For the $\text{Sc}^{45}(\alpha, t)\text{Ti}^{46}$ reaction $|\underline{k}_\alpha|$ differs enough from $|\underline{k}_t|$ that the minimum value of $|\underline{q}|R$ is greater than 1. Hence the condition $|\underline{q}|R = l$ can never be satisfied for the $l_p = 1$ proton transfers, and these transitions should be suppressed. Other evidence for the suppression of the $l_p = 1$ components of the mixed $l_p = 1$ and $l_p = 3$ transitions can be seen from the shapes of the (α, t) angular distributions. There are no distinguishing characteristics in, for example, the angular distributions for production of the first three states in Ti^{46} as shown in figure 5. This is in contrast to that observed in the (He^3, d) reaction where the $l_p = 1$ component can easily be observed at the forward angles.

Even though the energy resolution in the present experiment was not adequate for resolving discrete states above 3 MeV in Ti^{46} , an analysis of the angular distributions presented in figure 3, within the framework of current DWBA stripping reaction formalisms, seems reasonable because of the suppression of the $l_p = 1$ transitions and the selectivity of the (α, t) reaction for certain residual states. The data are all consistent and all angular distributions display the same basic shape.

For the transfer of a nucleon with l units of orbital angular momentum, it is customary to write the differential cross sections as (ref. 19)

$$\frac{d\sigma}{d\Omega} \propto \left(\frac{2J_f + 1}{2J_i + 1} \right) S_l \sigma_{\text{DWBA}} \quad (2)$$

If the isospin formalism is used, then S_l should be replaced by C^2S (ref. 20). Since the theoretical values of the S_l used in this analysis did not include the isospin factor, the form of the differential cross section in equation (2) will be used to determine experimental values of S_l . The spectroscopic factor S_l contains the structure information for the nuclei involved and is defined for single-particle wave functions as (ref. 7)

$$S_l = n \left[\left\langle \Psi_m^{J_f} \left| \left(\Psi_i \varphi^j \right)_m^{J_i} \right. \right\rangle \right]^2 \quad (3)$$

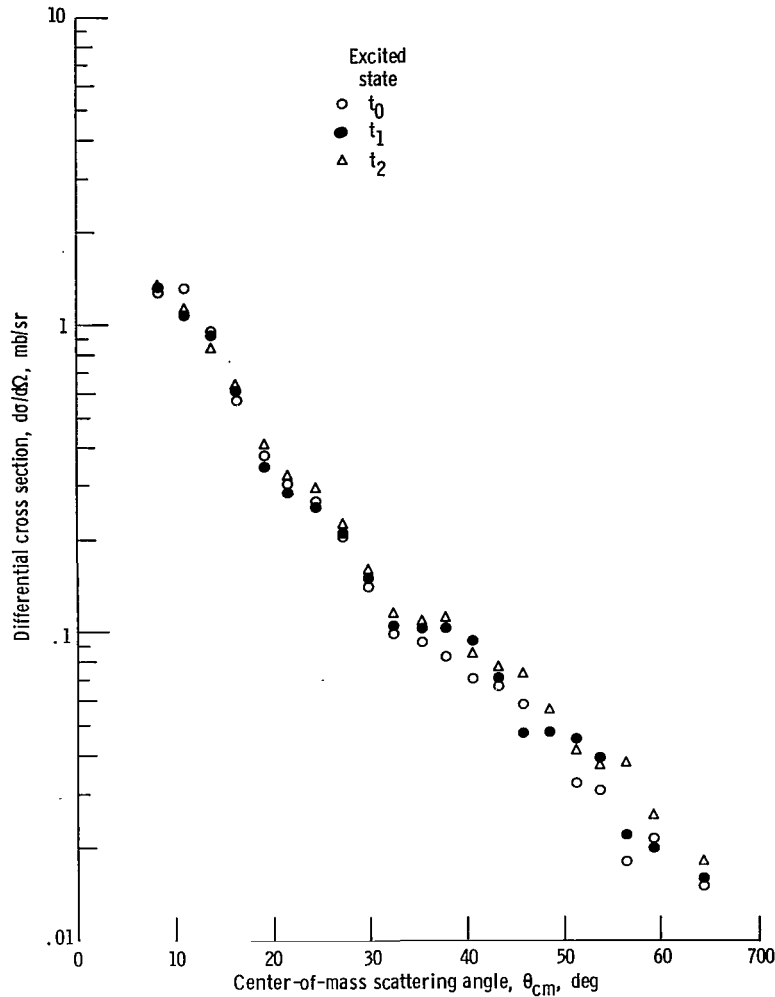


Figure 5. - Normalized angular distributions for t_0 , t_1 , and t_2 triton groups in the $\text{Sc}^{45}(\alpha, t)\text{Ti}^{46}$ reaction.

Equation (2) is a proportionality rather than an equality because the formalism involves an overlap integral for the dissociation of an alpha particle into a triton and proton, and this quantity is not normally calculated for the (α, t) reaction. This constant will be determined empirically by normalizing the $\text{Sc}^{45}(\alpha, t_0)\text{Ti}^{46}$ data to the $\text{Sc}^{45}(\text{He}^3, d_0)\text{Ti}^{46}$ data.

The DWBA formalism of Tobocman (ref. 21) was used for the description of σ_{DWBA} in equation (2). The numerical calculations employed the zero-range approximation for the nuclear interaction, noncut-off radius approximation for the radial integrals, and were made with the direct-reaction FORTRAN code written by Gibbs et al. (ref. 22). The wave functions for the incident and exit channels were generated using a Woods-Saxon potential of the form

$$V_C = \frac{V}{1 + e^x} - \frac{iW}{1 + e^{x'}}$$

where

$$x = \frac{r - r_0 A^{1/3}}{a}$$

$$x' = \frac{r - r'_0 A^{1/3}}{a'}$$

The potential parameters for the incident $\alpha + \text{Sc}^{45}$ system were obtained from calculations of the differential cross sections for the elastic scattering of 41-MeV alpha particles from Sc^{45} . The theoretical calculations determined those potential parameters which minimized the χ^2 function defined by

$$\chi^2 = \frac{1}{N} \sum_{i=1}^N \left(\frac{\sigma_i^{\text{exp}} - \sigma_i^{\text{theo}}}{\Delta \sigma_i^{\text{exp}}} \right)^2$$

TABLE IV. - OPTICAL MODEL PARAMETERS

Potential set	Particle	Real nuclear potential, V, MeV	Reduced nuclear radius for real potential, r_0 , fm	Nuclear diffuseness for real nuclear potential, a, fm	Imaginary nuclear potential, W, MeV	Reduced radius for imaginary nuclear potential, r'_0 , fm	Nuclear diffuseness for imaginary nuclear potential, a', fm	Coulomb radius, r_{oc} , fm	Goodness of fit, χ^2
1	Alpha	27.0	1.7	0.591	11.7	1.7	0.591	1.7	125
2		64.4	1.6	.538	14.3	1.6	.538	1.6	86
3		103.6	1.515	.544	17.5	1.515	.544	1.515	104
^a 4		200.2	1.395	.565	26.4	1.395	.565	1.395	144
5	Triton ^b	150.6	1.24	.678	25.0	1.45	.841	1.24	---

^aUsed in DWBA calculations.

^bTriton potential parameters were estimated from the 20 MeV-triton elastic scattering results of Hafele, et al. (ref. 23).

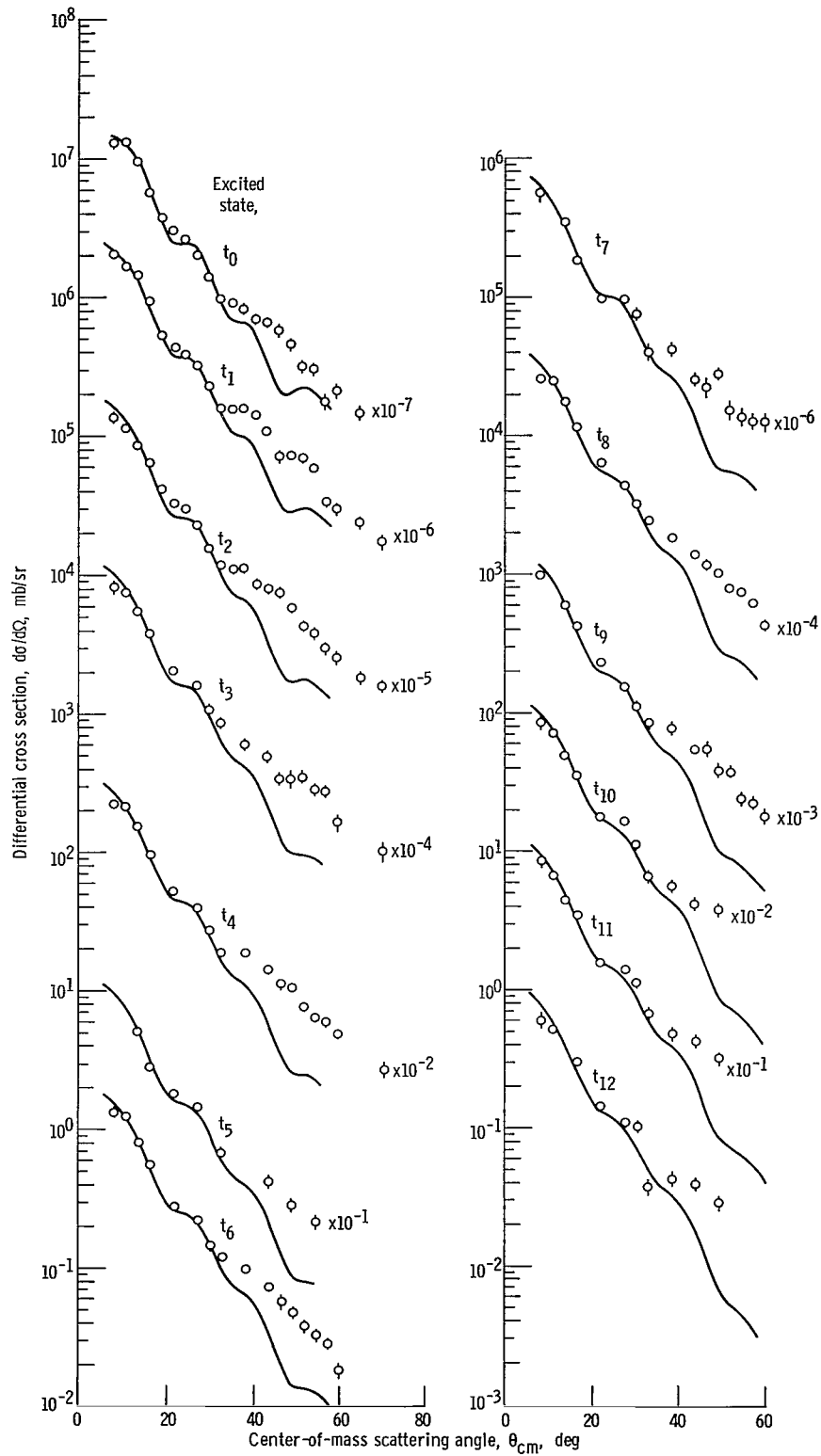


Figure 6. - Theoretical fits to triton angular distributions for $Sc^{45}(\alpha, t)Ti^{46}$ reaction using the DWBA calculations described in text.

Four sets of equivalent parameters are given in table IV. The calculation using the deep well parameters (set 4) is displayed along with the experimental results in figure 4. Since similar data were not available for the exit $t + \text{Ti}^{46}$ system, the triton optical model parameters were estimated from the 20-MeV triton elastic scattering results of Hafele et al. (ref. 23). The potential well depths were calculated from the expressions $V = 0.057 A + 148$ and $W = -0.097 A + 29.4$. This dependence of V and W on A for $52 \leq A \leq 116$ was deduced by Hafele et al. (ref. 23) using fixed geometrical parameters. The complete set of parameters is listed as set 5 in table IV.

The bound-state wave function for the captured proton was an eigenfunction of a Woods-Saxon Hamiltonian with eigenenergy equal to the binding energy of the proton in the residual nucleus. The potential did not contain a spin-orbit term. The radius and diffuseness parameters of the potential functions were 4.5 and 0.65 fermi (femtometer). The depth of the potential was chosen to reproduce the binding energy.

The numerical calculations employing the deep well optical model potential parameters (currently favored in the literature) for the incident $\alpha + \text{Sc}^{45}$ system are displayed in figure 6. Essentially equivalent fits can be obtained with any of the sets of optical model potential parameters listed in table IV if the cut-off radius calculation is used. We find, however, that for the deep well parameters the calculations are much less sensitive to choice of the cut-off radius and that the difference in magnitude and shape of the theoretical angular distributions for zero and nonzero cut-off calculations are less pronounced. The theoretical calculations were adjusted in magnitude by determining the normalization parameter γ which minimized the χ^2 function defined by

$$\chi^2 = \sum_{\theta=8^{\circ}}^{35^{\circ}} \left(\frac{\gamma \sigma_{\theta}^{\text{theo}} - \sigma_{\theta}^{\text{exp}}}{\Delta \sigma_{\theta}^{\text{exp}}} \right)^2$$

The theoretical fits are quite satisfactory in the angular region 8° to 35° and are reasonable at the larger angles. Relative spectroscopic strengths were extracted by assuming Barnard and Jones' value of 0.27 for the spectroscopic strength of the ground-state transition in the $\text{Sc}^{45}(\text{He}^3, d_0)\text{Ti}^{46}$ reaction. These spectroscopic strengths are listed in table V and are displayed graphically in figure 7. Some appropriate $l_p = 3$ spectroscopic strengths from the works of Broman and Pullen (ref. 8) and Barnard and Jones (ref. 9) are also shown. Broman and Pullen's data have been normalized to the ground-state data. In view of the uncertainties in the experimental data and the theoretical fits, the agreement between the spectroscopic strengths obtained from the (α, t) and (He^3, d) reactions is good. All spectroscopic strengths, with the possible exception of that for the t_8 transition, agree within the associated errors. The good agreement is probably

TABLE V. - SINGLE-PROTON-TRANSFER THEORETICAL SPECTROGRAPHIC STRENGTHS FOR
STRIPPING REACTION AS DEDUCED FROM McCULLEN, BYMAN, AND ZAMICK SINGLE-
PARTICLE WAVE FUNCTIONS FOR SCANDIUM-45 AND TITANIUM-46

Excitation, MeV	Final state spin	Spectroscopic factor, S	Spectroscopic strength, $\left(\frac{2J_f + 1}{2J_i + 1}\right) S$	Excitation, MeV	Final state spin	Spectroscopic factor, S	Spectroscopic strength, $\left(\frac{2J_f + 1}{2J_i + 1}\right) S$
0	0	2.0000	0.2500	5.6391	4	0.0012	0.0013
1.1009	2	1.3200	.8250	5.6761	3	.0690	.0609
2.1726	4	.3885	.4370	5.6966	7	.0534	.1001
2.7710	2	.3328	.2080	5.9327	8	0	0
3.2126	4	.00079	.00089	5.9423	7	.0720	.1350
3.2639	6	.3523	.5724	5.7980	2	0	0
3.6944	2	.1955	.1221	6.0965	4	.0533	.0599
3.7482	3	.0616	.0539	6.1339	5	.0205	.0281
3.9031	4	.8996	1.0120	6.2678	6	.0004	.0007
3.9966	1	.0641	.0240	6.4425	6	.0752	.1222
4.0224	5	.0005	.00069	6.5901	7	.0117	.0219
4.1870	6	.8517	1.3840	6.6614	5	.0046	.0064
4.8897	6	.0011	.0017	6.8694	1	.0032	.0012
4.9821	8	0	0	6.9170	6	.0059	.0097
5.1973	0	0	0	7.0542	3	0	0
5.2026	5	.0587	.0807	7.1207	0	.0003	0
5.2119	4	.0013	.0014	7.1236	2	.00041	.0003
5.4751	3	.0435	.0380	7.1894	4	.0061	.0069
5.4989	2	.0003	.00019	7.2550	6	.0237	.0386

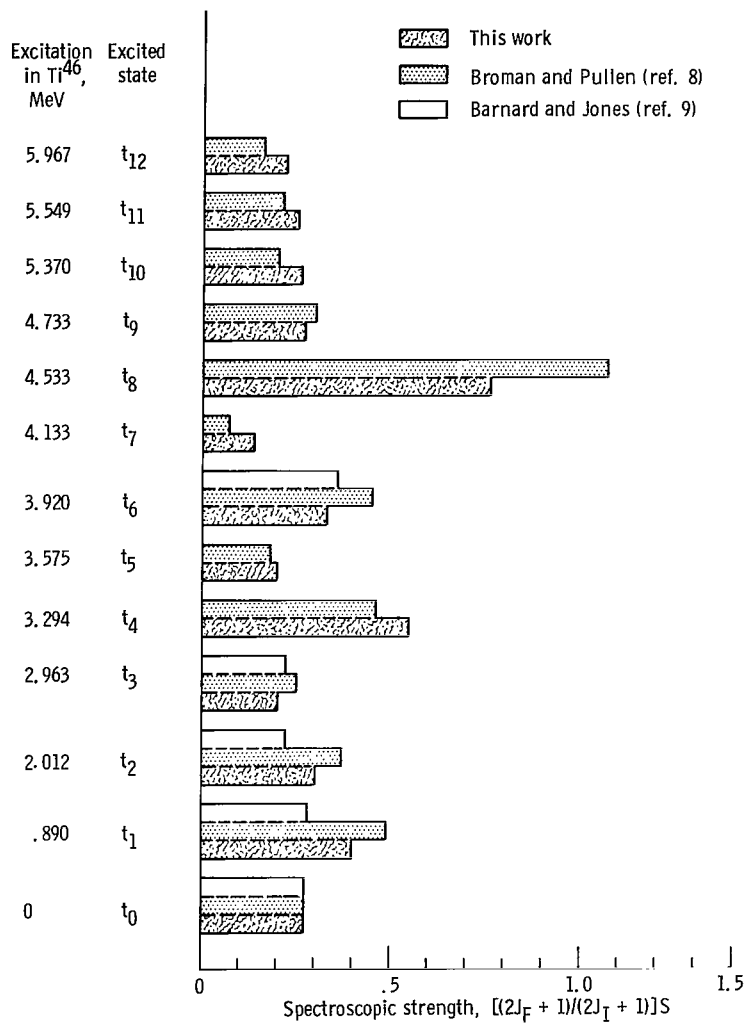


Figure 7. - Comparison of spectroscopic strengths for (α, t) and (He^3, d) reactions on Sc^{45} . Only $t_p = 3$ component of (He^3, d) spectroscopic strength is shown.

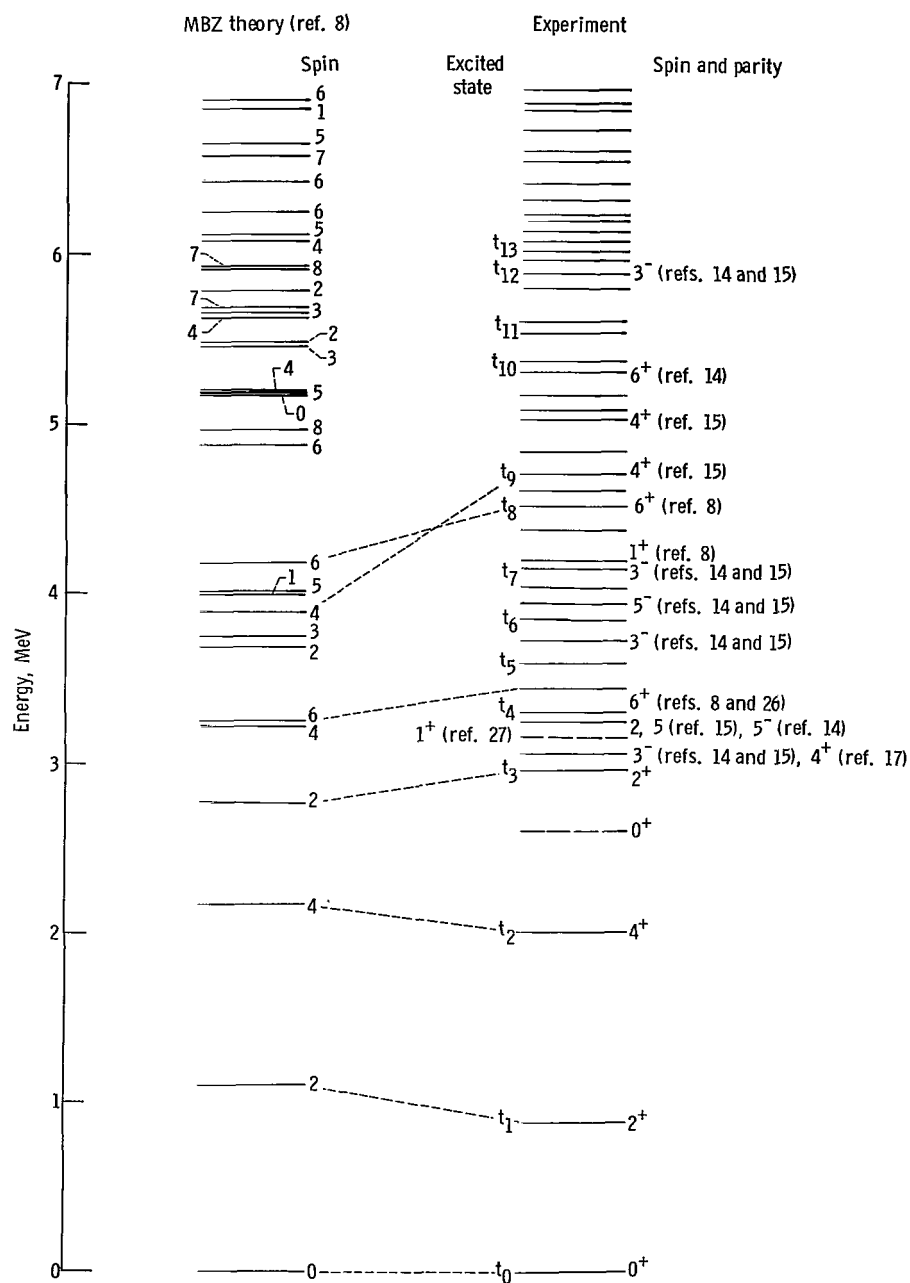


Figure 8. - The energy levels of titanium-46 as reported by Broman and Pullen (ref. 8). The t_i notation indicates those levels studied in the $\text{Sc}^{45}(\alpha, t)\text{Ti}^{46}$ reaction. The two levels shown as dashed lines were not reported by Broman and Pullen but have been seen by several other investigators. The interconnecting dashed lines indicate those levels which can possibly be identified with the predictions of McCullen et al.

due to the large proton orbital angular momentum transfers ($l_p = 3$) which, for the (α, t) reaction, favor the direct reaction mechanism (ref. 3).

The wave functions of the McCullen, Bayman, and Zamick (ref. 7) (hereafter referred to as MBZ) for Sc^{45} and Ti^{46} were used in the theoretical calculation of the spectroscopic factors. They assume that these nuclei are described by wave functions composed of a calcium-40 (Ca^{40}) core plus Z-20 protons and N-20 neutrons in the $1f_{7/2}$ shell. Experimental evidence from the $\text{Sc}^{45}(\text{He}^3, d)\text{Ti}^{46}$ reaction and comparison of theoretical and experimental energy spectra (fig. 8) indicates that this is only an approximation since the wave function for many of the excited states of Ti^{46} clearly contain admixtures of $2p_{3/2}$ configurations. They write the Ti^{46} and Sc^{45} wave functions in states α and β as

$$\Psi_{1234, P_1 P_2}(\text{Ti}^{46} \alpha J_f M) = \sum_{L_p L_n \nu_n} D^{\alpha J_f} (L_p L_n \nu_n) \left[\Psi_{12} j^2 L_p \Psi_{1234} j^4 \nu_n L_n \right]_M^{J_f} \quad (7)$$

$$\Psi_{1234, P_1}(\text{Sc}^{45} \beta J_i M) = \sum_{\nu'_n L'_n} C^{\beta J_i} (\nu'_n L'_n) \left[\Psi_{1234} (j^4 \nu'_n L'_n) \Psi_1(j) \right]_M^{J_i} \quad (8)$$

Following MBZ, the theoretical spectroscopic factor for the $\text{Sc}^{45}(\alpha, t)\text{Ti}^{46}$ reaction becomes

$$S = 2 \left[\sum_{L_{p1} \nu_n L_n} (-1)^{L_n} D^{\alpha J_f} (L_{p1} \nu_n L_n) C^{1 J_i} (\nu_n L_n) U(j j J_f L_n; L_{p1} J_i) \right]^2 \quad (9)$$

where U is the normalized Racah coefficient in Jahn's notation (ref. 24). Results obtained for the evaluation of equation (9) for the first $\nu 8$ states of Ti^{46} predicted by the MBZ model are shown in table V. The numerical values of the $C^{1 J_i}$ and $D^{\alpha J_f}$ were taken from reference 25. For excitations above ν MeV in Ti^{46} , the few spin and parity assignments are very tentative, and it is thus impossible to identify which states cor-

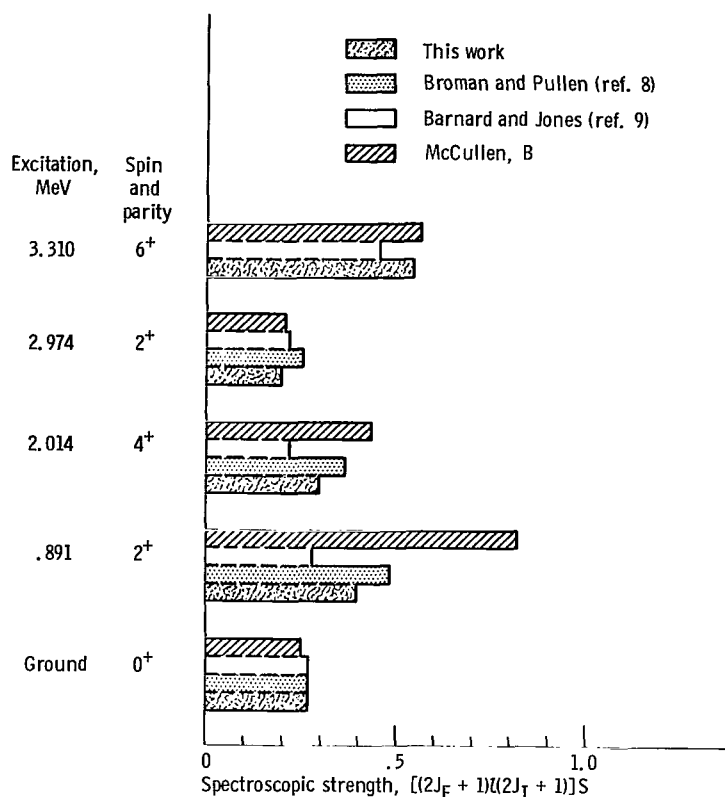


Figure 9. - Comparison of the theoretical spectroscopic strengths calculated from the scandium-45 and titanium-46 single-particle wave functions of McCullen, Bayman, and Zamick with the experimental results of references 8 and 9 and this work.

to the MBZ predictions. The spin and parity of the first four states of Ti^{46} are predicted by the MBZ model, and the level at 3.310 MeV, which has been given a tentative assignment (ref. 26) of 6^+ , appears to be the first 6^+ level predicted by the MBZ model. The MBZ spectroscopic factors are displayed along with the experimental values in figure 9. The agreement is quite satisfactory especially for those transitions shown to be pure $l_p = 3$ angular momentum transfer in the (He^3, d) reaction. The good agreement between the MBZ and experimental spectroscopic factors for the 3.310-MeV state supports the contention that the spin and parity of this state is 6^+ .

It is, of course, difficult to make definite spin and parity assignments to the states of Ti^{46} on the basis of a comparison of the experimental and theoretical spectroscopic strengths just presented. However, table V shows particularly large spectroscopic strengths for a few transitions. It may be possible, then, to make some corroboration of a tentative assignment or some reasonable speculation for an assignment.

Broman and Pullen (ref. 8) have suggested that the states at 3.310, 4.206, and 4.533 MeV have spin and parity 6^+ , 1^+ , and 6^+ . The reason being that these correspond to

pure $l_p = 3$ transitions, and production of a 1^+ or 6^+ state by $l_p = 1$ angular momentum transfer is forbidden by the selection rule for angular momentum. These states could correspond to the 6^+ , 1^+ , and 6^+ states at 3.2639, 3.9966, and 4.1870 MeV in the MBZ model.

As discussed earlier, the MBZ spectroscopic strength for the first 6^+ state is in good agreement with the experimental value for the 3.310-MeV state. The MBZ spectroscopic strength for the first 1^+ state is much lower than the experimental value for the 4.206-MeV state, so any verification of a tentative 1^+ assignment is dangerous. Since Lewis et al. (ref. 27) have identified the state at 3.17 MeV as being 1^+ , it would seem that this is a better candidate for the MBZ 1^+ state at 3.9966 MeV since the next 1^+ state in the MBZ model occurs at 6.8694 MeV. The small MBZ spectroscopic strength for this state at 3.9966 MeV would explain why this state was not excited in either the high-resolution study of the $\text{Sc}^{45}(\text{He}^3, d)\text{Ti}^{46}$ reaction by Broman and Pullen (ref. 8) or the $\text{Sc}^{45}(\alpha, t)\text{Ti}^{46}$ reaction in this study. The MBZ spectroscopic strength for the second 6^+ level is the largest of all the theoretical values and is in good agreement with the experimental value for the 4.533-MeV state. We can then substantiate Broman and Pullen's assignments to the 6^+ states (ref. 8), but we tend to disagree with the 1^+ assignment.

Figure 8 shows a number of odd-parity, odd-integral spin states. These have been identified as collective states by means of inelastic scattering of alpha particles from Ti^{46} (refs. 14 and 15). Several of these states between 3.6- and 4.2-MeV excitation are excited both by the (α, t) and (He^3, d) reactions. Since odd parity states are not predicted by the MBZ model, we can make no statement about these assignments. These same inelastic scattering studies have yielded a tentative 4^+ assignment for the 4.723 MeV state (ref. 15). This state is strongly excited in both the (He^3, d) and (α, t) experiments. The MBZ spectroscopic strength for the third 4^+ state at 3.9031 MeV is 1.01. This is, however, still a factor of 3 to 5 larger than the (α, t) and (He^3, d) spectroscopic strengths. Thus because of this large difference in the theoretical and experimental spectroscopic strengths and energies, the corroborating evidence for this 4^+ assignment is weak.

Several states above 5-MeV excitation are strongly excited in both the (α, t) and (He^3, d) reactions. None of these states have been given spin assignments, so nothing quantitative can be said about them. The MBZ spectroscopic strengths (table V) for this energy region are largest for the higher spins. Probably, then, these strongly excited states have spins in the range 3 to 7.

CONCLUSION

Transitions to the states of Ti^{46} via the $\text{Sc}^{45}(\alpha, t)\text{Ti}^{46}$ reactions have been shown to proceed primarily by $l_p = 3$ proton angular momentum transfer since the distorted

wave Born approximation calculations for the stripping of a proton from the incident alpha particle yield reasonable fits to the triton angular distributions. Spectroscopic factors deduced from the distorted wave Born analysis compare favorably with those deduced from a similar analysis of the $\text{Sc}^{45}(\text{He}^3, \text{d})\text{Ti}^{46}$ reaction. Theoretical spectroscopic factors calculated in this work from the McCullen, Bayman, and Zamick model for Ti^{46} are in reasonable agreement with this experiment. The good overall agreement between theory and experiment for both the (α, t) and (He^3, d) reactions on Sc^{45} indicates that the (α, t) reaction is a useful tool for nuclear spectroscopy where several units of orbital angular momentum are transferred.

Lewis Research Center,
National Aeronautics and Space Administration,
Cleveland, Ohio, January 28, 1969,
129-02-04-06-22.

REFERENCES

1. Yntema, J. L.: The (α, t) Reaction on Nuclei. Proceedings of the Rutherford Jubilee International Conference, Manchester, 1961. J. B. Birks, ed., Academic Press, 1961, pp. 513-514.
2. Jahr, R.: Study of the Reactions $\text{F}^{19}(\alpha, \text{t})\text{Ne}^{20}$ at 18.5 MeV and $\text{F}^{19}(\text{He}^3, \text{d})\text{Ne}^{20}$ at 13.0 MeV. Phys. Rev., vol. 129, no. 1, Jan. 1, 1963, pp. 320-323.
3. Armstrong, D. D.; Blair, A. G.; and Thomas, H. C.: (He^4, t) Reaction on Medium-Weight Nuclei. Phys. Rev., vol. 155, no. 4, Mar. 20, 1967, pp. 1254-1260.
4. Hansen, Luisa F.; Lutz, H. F.; Stelts, Marion L.; Vidal, Jose G.; and Wesolowski, Jerome J.: Study of the (α, t) Reaction in F^{19} . Phys. Rev., vol. 158, no. 4, June 20, 1967, pp. 917-924.
5. Blair, Allen G.: Complex Single-Nucleon Stripping and Pickup Reactions (α, t) , (d, He^3) , etc. Nuclear Spectroscopy with Direct Reactions. II. Proceedings. F. E. Throw, ed. Rep. ANL-6878, Argonne National Lab., 1964, pp. 115-138.
6. Bingham, C. R.; and Halbert, M. L.: $^{92}\text{Zr}(\text{}^3\text{He}, \text{}^3\text{He}') \text{ and } ^{92}\text{Zr}(\text{}^3\text{He}, \alpha) \text{ with } 51\text{-MeV } ^3\text{He}$. Phys. Rev., vol. 158, no. 4, June 20, 1967, pp. 1085-1093.
7. McCullen, J. D.; Bayman, B. F.; and Zamick, Larry: Spectroscopy in the Nuclear $1f_{7/2}$ Shell. Phys. Rev., vol. 134, no. 3B, May 11, 1964, pp. 515-538.
8. Broman, Lars; and Pullen, D. J.: Level Structure of ^{46}Ti . Nucl. Phys., vol. A110, 1968, pp. 161-175.

9. Barnard, R. W.; and Jones, G. D.: A Study of ^{46}Ti by the $^{45}\text{Sc}(^3\text{He}, d)^{46}\text{Ti}$ and $^{46}\text{Ti}(p, p')^{46}\text{Ti}$ Reactions. Nucl. Phys., vol. A111, 1968, pp. 17-38.
10. Goulding, Fred S.; Landis, Donald A.; Cerny, Joseph, III; and Pehl, Richard H.: A New Particle Identifier Technique for $Z = 1$ and $Z = 2$ Particles in the Energy Range >10 MeV. IEEE Trans. on Nucl. Sci., vol. NS-11, no. 3, July 1964, pp. 388-398.
11. Nuclear Data Group of Oak Ridge National Lab.: Nuclear Data Sheets. National Academy of Sciences - National Research Council, Nov. 1964.
12. Yntema, J. L.: (d, t) Reaction on the Titanium Isotopes. Phys. Rev., vol. 127, no. 5, Sept. 1, 1962, pp. 1659-1663.
13. Kashy, E.; and Conlon, T. W.: Shell-Model States and Configuration Mixing in the Ti Isotopes by the (p, d) Reaction. Phys. Rev., vol. 135, no. 2B, July 27, 1964, pp. 389-401.
14. Bruge, G.; Faivre, J. C.; Farraggi, H.; Vallois, G.; Bussiere, A.; and Roussel, P.: Diffusion Inelastique des Particules α par les Noyaux de la Region $N = 28$. Phys. Letters, vol. 20, no. 3, Feb. 15, 1966, pp. 293-295.
15. Yntema, J. L.; and Satchler, G. R.: Scattering of 43-MeV Alpha Particles by the Titanium Isotopes. Phys. Rev., vol. 161, no. 4, Sept. 20, 1967, pp. 1137-1147.
16. Church, D. J.; Horoshko, R. N.; and Mitchell, G. E.: Study of Low-Lying States in ^{46}Ti , ^{48}Ti , and ^{54}Fe . Phys. Rev., vol. 160, no. 4, Aug. 20, 1967, pp. 894-902.
17. Mo, J. N.; Twin, P. J.; and Willmott, J. C.: An Investigation into the Lower Excited States of ^{48}Ti . Nucl. Phys., vol. 89, 1966, pp. 686-696.
18. Butler, S. T.; and Hittmair, O. H.: Nuclear Stripping Reactions. John Wiley & Sons, Inc., 1957, pp. 5-6.
19. Bassel, R. H.: Normalization of and Finite-Range Effects in $(^3\text{He}, d)$ and (t, d) Reactions. Phys. Rev., vol. 149, no. 3, Sept. 23, 1966, pp. 791-797.
20. Glendenning, Norman K.: Nuclear Stripping Reactions. Ann. Rev. Nucl. Sci., vol. 13, 1963, pp. 191-260.
21. Tobocman, W.: Theory of Direct Nuclear Reactions. Oxford Univ. Press, London, 1961.
22. Gibbs, W. R.; Madsen, V. A.; Miller, J. A.; Tobocman, W.; Cox, E. C.; and Mowry, L.: Direct Reaction Calculation. NASA TN D-2170, 1964.
23. Hafele, J. C.; Flynn, E. R.; and Blair, A. G.: Triton Elastic Scattering. Phys. Rev., vol. 155, no. 4, Mar. 20, 1967, pp. 1238-1245.

24. Jahn, H. A.: Theoretical Studies in Nuclear Structure. II. Nuclear d^2 , d^3 and d^4 Configurations. Fractional Parentage Coefficients and Central Force Matrix Elements. Proc. Roy. Soc. (London), Ser. A, vol. 205, no. 1081, Feb. 7, 1951, pp. 192-237.
25. McCullen, J. D.; Bayman, B. F.; and Zamick, Larry: Wave Functions in the $1f_{7/2}$ Shell. Princeton Univ. (AEC Rep. NYO-9891), June 1964.
26. Dubois, J.; and Maripuu, S.: Radiative Proton Capture in Sc^{45} . Arkiv Fysik, vol. 24, 1963, pp. 127-149.
27. Lewis, C. W.; Mo, J. N.; Monohan, C. F.; Thomas, M. F.; and Twin, P. J.: A Low Lying Spin 1 State in Ti^{46} . Phys. Letters, vol. 22, no. 4, Sept. 1, 1966, pp. 476-477.

FIRST CLASS MAIL

POSTMASTER: If Undeliverable (Section 158
Postal Manual) Do Not Return

"The aeronautical and space activities of the United States shall be conducted so as to contribute . . . to the expansion of human knowledge of phenomena in the atmosphere and space. The Administration shall provide for the widest practicable and appropriate dissemination of information concerning its activities and the results thereof."

— NATIONAL AERONAUTICS AND SPACE ACT OF 1958

NASA SCIENTIFIC AND TECHNICAL PUBLICATIONS

TECHNICAL REPORTS: Scientific and technical information considered important, complete, and a lasting contribution to existing knowledge.

TECHNICAL NOTES: Information less broad in scope but nevertheless of importance as a contribution to existing knowledge.

TECHNICAL MEMORANDUMS: Information receiving limited distribution because of preliminary data, security classification, or other reasons.

CONTRACTOR REPORTS: Scientific and technical information generated under a NASA contract or grant and considered an important contribution to existing knowledge.

TECHNICAL TRANSLATIONS: Information published in a foreign language considered to merit NASA distribution in English.

SPECIAL PUBLICATIONS: Information derived from or of value to NASA activities. Publications include conference proceedings, monographs, data compilations, handbooks, sourcebooks, and special bibliographies.

TECHNOLOGY UTILIZATION PUBLICATIONS: Information on technology used by NASA that may be of particular interest in commercial and other non-aerospace applications. Publications include Tech Briefs, Technology Utilization Reports and Notes, and Technology Surveys.

Details on the availability of these publications may be obtained from:

SCIENTIFIC AND TECHNICAL INFORMATION DIVISION
NATIONAL AERONAUTICS AND SPACE ADMINISTRATION
Washington, D.C. 20546